香港天文台
HONG KONG OBSERVATORY

Reprint 645

Simulation of Distant Earthquakes Affecting Hong Kong

K. Megawati [1], W.T. Wong, L.S. Chan [2], A.M. Chandler [1] & Y.W. Chan

3rd International Conference on Continental Earthquakes,

Beijing, China, 12-14 July 2004

[1] *Centre for Earthquake Engineering Research (CEER) and Department of Civil Engineering, The University of Hong Kong*

[2] *Centre for Earthquake Engineering Research (CEER) and Department of Earth Sciences, The University of Hong Kong*

SIMULATION OF DISTANT EARTHQUAKES AFFECTING HONG KONG

K. Megawati[1], W.T. Wong[2], L.S. Chan[3], A.M. Chandler[1] and Y.W. Chan[2]

[1]Centre for Earthquake Engineering Research (CEER) and Department of Civil Engineering, The University of Hong Kong, Pokfulam Road, Hong Kong
[2]Hong Kong Observatory, 134A Nathan Road, Kowloon, Hong Kong
[3]Centre for Earthquake Engineering Research (CEER) and Department of Earth Sciences, The University of Hong Kong, Pokfulam Road, Hong Kong

ABSTRACT

Hong Kong is located in South-eastern China, which is considered an intraplate region with moderate seismic activity. Traditionally, seismic risk to structures in Hong Kong was considered to be insignificant, but due to rapid construction of high-rise buildings, complex infrastructures and industrial facilities in the last 50 years, the seismic risk has increased tremendously. Potential earthquakes in the near field and far field of Hong Kong contribute differently to the ground-motion hazard, depending on the natural period of concern. Earthquakes at distances smaller than 100 km contribute most to the hazard level within a natural-period range less than 0.8 s, while the contribution from large-magnitude distant earthquakes, located 150 to 400 km from Hong Kong, becomes dominant for natural periods larger than 1 s. Since the majority of buildings in Hong Kong are high-rise structures, large-magnitude distant intraplate earthquakes are expected to be the main source of concern. This paper attempts to identify the controlling earthquake in the far field of Hong Kong and to investigate the characteristics of ground motion that may be generated by the earthquake. This is achieved through a series of ground motion simulations. Ground motions from several small-magnitude earthquakes in Nanao, Yangjiang and Heyuan recorded in Hong Kong recently are utilised to validate the regional crustal structure and the synthetic seismogram method adopted. Random rupture models, considering the uncertainties in rupture directivity, slip distribution, presence of asperities, rupture velocity and dislocation rise-time, are constructed based on a range of seismologically possible parameters. Ground motion time-histories and response spectra associated with the uncertainties in the rupture process are then presented in a form suitable for structural design. The forward rupture directivity is found to be the main factor responsible for generating ground motion with a large long-period pulse. The characteristics of the resulting ground motions provide essential information for refining the seismic hazard levels of Hong Kong, especially in the long natural-period range.

INTRODUCTION

It has been recognized that urban areas located at large distances from tectonic plate margins, broadly categorised as low- to moderate-seismicity regions, may also be affected by earthquake tremors. Hong Kong is one example of such region in Asia. It is located in South-eastern China, which is considered an intraplate region with moderate seismic activity level. Traditionally, seismic risk to structures in Hong Kong was considered low. In the first half of the last century, the population of the city had not reached one million, and the majority of the buildings were simple low-rise structures. However, the city changed dramatically in the second half of the century, in line with the rapid economic growth in Asia and the Pacific. Hong Kong has developed into a modern metropolis with a population of 6.8 million, large concentrations of high-rise buildings, complex infrastructures, industrial facilities, and a significant proportion of reclaimed land. Therefore, although the seismic hazard of the city remains moderate, the seismic risk, in terms of damage potential to structures, loss of lives, assets, businesses and services, has increased tremendously compared to the situation 50 years ago.

Following the above consideration, the Government of the Hong Kong Special Administrative Region (HKSAR) has embarked on a comprehensive assessment of seismic issues. The Buildings Department (BD) in 2002 commissioned a consultancy study to investigate thoroughly the seismic hazard of the territory and the seismic risk to its buildings and infrastructures. The study has shown that potential earthquakes in the near field and far field of Hong Kong contribute differently to the ground-motion hazard depending on the natural period of concern. The de-aggregation of the uniform hazard spectra (UHS) resulting from a probabilistic seismic hazard assessment enables the most dominant event giving rise to the ground-motion hazard at any particular natural period to be determined. It indicates that earthquakes at distances smaller than 100 km contribute most to the hazard level within a natural period range less than 0.8 s, while the contribution from large-magnitude distant earthquakes, located 150 to 400 km from Hong Kong, becomes dominant for natural periods larger than 1 s. Since the majority of buildings in Hong Kong are high-rise structures, large-magnitude distant intraplate earthquakes are expected to be the main source of concern due to the damage potential to the building stock in the city.

It is therefore crucial to understand the characteristics of ground motions that may be generated by such far-field earthquakes. The key factors that need to be examined are not limited to the peak ground accelerations and velocities, but they should also include the shape and ordinates of the corresponding response spectra, the duration of the ground shaking and other special features that may arise from the rupture mechanism of the earthquakes.

The objectives of the present research are to identify the controlling earthquake in the far field of Hong Kong and to investigate the characteristics of the ground motion that may be generated by such an earthquake. This is achieved through a series of ground motion simulations of various scenario earthquakes in the far field. The ground motions of small-magnitude distant earthquakes recorded in Hong Kong recently are utilised to validate the regional crustal structure and the synthetic seismogram method adopted. Random rupture models, considering the uncertainties in rupture directivity, slip distribution, presence of asperities, rupture velocity and dislocation rise-time, are constructed based on a range of seismologically possible parameters. Ground motion time-histories and response spectra associated with the uncertainties in the rupture process are then presented in a form suitable for structural design consideration.

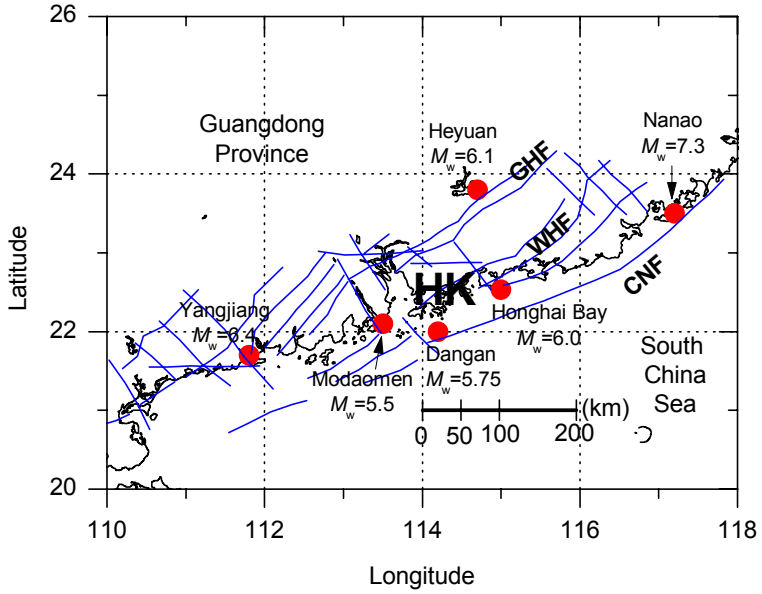

Figure 1. Major fault systems in the Hong Kong Region with identified historical earthquakes. CNF: Changle – Nanao Fault, WHF: Wuhua – Haifeng Fault, GHF: Guangzhou – Heyuan Fault.

SEISMOTECTONICS OF THE HONG KONG REGION

Regional Tectonic Setting

The study area bounded by latitudes 20°N – 26°N and longitudes 110°E – 118°E (Figure 1), is referred to as the "Hong Kong Region". The region is part of the South China Maritime Fold Belt that was formed predominantly during the subduction of an ancient plate along the eastern coast of the South China Block about 160-90 m.y. ago [Wang and Lu, 1997]. Fault systems are well developed in the coastal areas of the Guangdong and Fujian provinces. The most prominent fault systems in the area are trending northeast, including the Changle-Nanao Fault (CNF) that runs along the coastline of South China, the Wuhua-Haifeng Fault (WHF) extending from Hong Kong to Wuhua, and the Guangzhou-Heyuan Fault (GHF) farther to the north (Figure 1). The northwest-trending faults in the region are less prominent but appear to be younger than the northeast trending ones based on their crosscutting relationship.

Geodetic measurements from the GEODYSSEA project during 1994 – 1998 have identified the existence of the Sunda Block, which exhibits a distinct differential motion with respect to the Eurasian plate [Wilson *et al*, 1999]. Since the Sunda Block includes the South China Sea, the relative motion between the Sunda Block and Eurasia must also yield an effect on the continental margin of China. The kinematic solutions have revealed plausibly a right-lateral motion between the two tectonic blocks [Pubellier, 1998]. Such relative motion must be absorbed by the coastal faults along the Guangdong and Fujian provinces. The inferred sense of motion is consistent with the observed focal plane mechanism of recent earthquakes in the area.

Seismic Activities

Hong Kong lies within the southeast coastal seismic belt of China, where strong earthquakes have occurred in the past. Over the last 1000 years, more than 46 earthquakes with magnitudes greater than 4.75, have occurred within a distance of 350 km from Hong Kong. Eleven of these earthquakes had magnitudes greater than 6 [Geotechnical Control Office, 1991]. The Guangdong coastal fault zone is the most significant seismic energy release zone. At least four major earthquakes occurring along this seismic zone have reportedly been felt in Hong Kong: Nanao earthquake in 1600 (M_w 7, R = 319 km), Dangan islands earthquake in 1874 (M_w 5.75, R = 30 km), Honghai Bay earthquake in 1911 (M_w 6, R = 85 km), and Nanao earthquake in 1918 (M_w 7.3, R = 338 km). R indicates the distance from the epicentre, shown in Figure 1, to the headquarters of the Hong Kong Observatory (HKO). The 1918 Nanao earthquake caused the strongest tremor ever felt in Hong Kong, resulting in some minor damage to masonry buildings. The intensities reported ranged from VI to VII on the Modified Mercalli Intensity (MMI) scale. Based on the instrumental earthquake record of Guangdong Province for the duration 1970-1995, the return period for large events within the entire southeast coastal seismic belt of China is estimated to be about 400 years [Chan and Zhao, 1996].

Earthquakes in the onshore region are distributed in a broad belt about 300 km wide that runs parallel to the coast of South China. Within this belt, most earthquake activities are concentrated in two regions, namely Heyuan and Yangjiang. Earthquakes that occurred within these two regions account for about 80% of the recorded events onshore. The largest events in these two regions are the reservoir-triggered Heyuan earthquake in 1962 (M_w 6.1, R = 174 km) and the Yangjiang earthquake in 1969 (M_w 6.4, R = 254 km). Their epicentres are also depicted in Figure 1. The NW-trending faults are of a smaller scale, with a notable event occurring in Modaomen (Macau) in 1905 (M_w 5.5, R = 85 km).

The descriptions of the historical earthquakes illustrate the complexity of the seismic activities in the region, where the main threats to Hong Kong may arise from both near-field (R < 100 km) and far-field (R = 100 – 400 km) intraplate earthquakes. This paper, however, will deal with the seismic hazards arising from the far-field earthquakes, which control the design of long-period structures. On the other hand, the design of short-period structures may be controlled by smaller magnitude earthquakes in the near-field region, such as the eastern coast of Lantau Island, Dangan Island and Honghai Bay, which will be the subject of a future paper.

SEISMIC MONITORING NETWORK IN HONG KONG

Earthquake monitoring in Hong Kong began in 1921 when a set of 3-component long-period seismographs was installed at the headquarters of the HKO to detect distant earthquakes. In 1979, a network of three short-period seismographs was set up in the territory to determine the locations and magnitudes of local earthquakes. The short-period seismograph network was upgraded in 1997 to a digital network that included eight seismograph stations scattered over the territory of Hong Kong [Tam *et al*, 1997]. These stations are located at Cape D'Aguilar, Cheung Chau, Keung Shan, Lead Mine Pass, Luk Keng, Siu Lam, Tsim Bei Tsui and Yuen Ng Fan (Figure 2). The installation sites were so selected that the seismometers were placed on good bedrock with low background noise and the baselines were maximised for accurate epicentre determination.

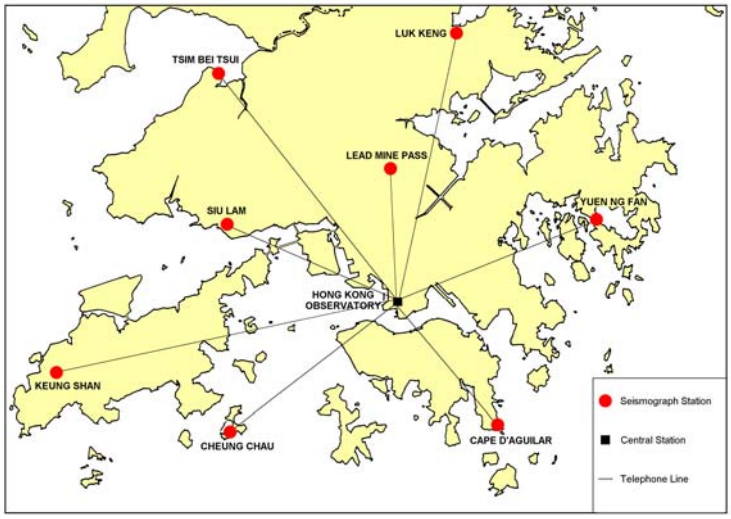

Figure 2. Seismic station network of Hong Kong.

The seismometers installed at the seismograph stations are piezoelectric sensors that are suitable for installation in boreholes. They have a dynamic range of about 100 dB with a frequency response of 1 to 30 Hz, and are capable of detecting ground motions with displacement as small as 1 nanometre (10^{-9} m). Apart from Tsim Bei Tsui where the seismometer is placed on a concrete plinth, the seismometers at all other stations are contained within plastic chambers set into concrete on bedrock in seismic pits. At Lead Mine Pass and Keung Shan, the seismometers are deployed in boreholes of 24 and 33 metres deep, respectively, to improve the signal-to-noise conditions. The seismometers at Tsim Bei Tsui and Yuen Ng Fan are 3-component instruments, while single vertical-component seismometers are deployed at the other stations that provide both velocity and acceleration output for seismic signals.

Digital data communication technology is employed in the seismograph network to enable real-time transmission of seismic data from the seismograph stations to the central data processing unit at the headquarters of the HKO for earthquake analysis. In 2003, the telemetry units and central data processing unit were replaced by a PC-based system that facilitated maintenance and worked on a higher sampling rate.

Signals from the seismometers are digitized at the seismograph stations with a 24-bit digitiser at a rate of 100 samples per second. A Global Positioning System receiver at each station provides time marks to the seismic signals. The data are transmitted through dedicated telephone lines at a baud rate of 9600 to the central data processing unit at the headquarters. The central data processing unit automatically calculates the short-term average and the long-term average of seismic signals of each station. If the ratios of these averages for any three stations exceed the pre-set trigger level simultaneously, the seismic signals of all the stations would be automatically saved into an event file for earthquake analysis. The SeisAn software package [Havskov and Ottemöller, 2003], with automatic phase picking and magnitude calculation capabilities, is used for initial determination of earthquake parameters including position and depth of the epicentre, and magnitude of the earthquake.

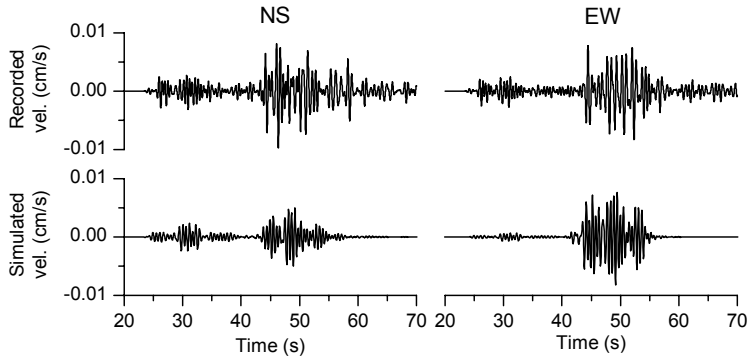

Figure 3. The recorded and simulated horizontal ground velocities of an earthquake (M_w 4.9) occurring in Heyuan on 20 August 1999.

Table I. Crustal structure of the coastal region of Hong Kong.

Layer	H (km)	v_P (km/s)	v_S (km/s)	ρ (t/m^3)	Q_P	Q_S
Sedimentary hard-rock	0.2	4.0	2.1	2.4	200	100
Upper crust	10.0	6.0	3.4	2.7	500	250
Middle crust	11.0	6.6	3.7	2.9	700	350
Lower crust	10.0	7.2	4.0	3.1	900	450
Mantle	∞	8.2	4.7	3.4	1000	500

H = layer thickness; v_P = P-wave velocity; v_S = S-wave velocity; ρ = mass density; Q_P = quality factor of P wave, Q_S = quality factor of S wave

VALIDATION OF REGIONAL CRUSTAL STRUCTURE

From the establishment of the Hong Kong digital seismic network in 1997 to December 2003, the network has recorded ground motions from numerous earthquakes in Heyuan, Yangjiang and Nanao, with magnitudes ranging from 3.3 to 4.9. The majority of the ground motions were weak but nevertheless with good signal-to-noise ratio. One of the strongest ground tremors that have been recorded by the digital network is an earthquake with an M_w of 4.9 occurring in Heyuan on 20 August 1999. The horizontal ground velocities of this earthquake recorded at the Tsim Bei Tsui station (R = 162 km) are shown in the upper panels of Figure 3, in the NS and EW directions. The records have been baseline corrected and filtered with a passing band of 1 – 2 Hz to remove high-frequency noise. The time 0 s refers to the rupture initiation time.

Ground motions of potential large-magnitude earthquakes in the far field of Hong Kong are to be estimated using synthetic seismograms. The ground motion simulations used in this study follow the reflectivity method developed by Kohketsu [1985], with propagator matrices of Fuchs [1968]. The seismic source is modelled as a single dislocation point source, whose source time function is approximated by a ramp function. The rise time of the function is determined from stress drop, according to the relationship proposed by Somerville *et al* [1987]. The crustal structure is modelled as a horizontally layered medium, where the structure is extracted from the global crustal model CRUST 2.0 [Laske *et al*, 2000], which is a 2^o x 2^o global model for the Earth's crust based on seismic refraction data published in the period of 1948 – 1995. The crustal structure of the coastal region bounded by latitudes 22^oN – 24^oN and longitudes 114^oE – 118^oE is summarised in Table I.

The appropriateness of the source and path modelling plays an important role in obtaining reliable results. Therefore, the reliability of the regional crustal model from CRUST 2.0 has to be examined first by observing the capability of the model to reproduce the ground motions of the small-magnitude earthquakes recorded by the HKO seismic stations. The panels in the bottom row of Figure 3 show the simulated ground velocities of the event in the NS and EW directions. The focal depth, strike and dip of the fault plane are 15 km, N45^{o}E and 60^{o}, respectively. The rake angle of the slip is taken to be -90^{o}, indicating a normal-slip earthquake, which is common in reservoir-triggered events. The source rise-time is calculated to be 0.80 s, assuming a stress drop of 100 bars [Somerville *et al*, 1987]. The lower and upper cut-off frequencies of the simulation are 1 and 2 Hz, respectively, which are set to be compatible with the recorded data. The first arrivals of the P- and S-waves occur 24 s and 43 s, respectively, after the rupture initiation. The simulated waveforms agree well with the recorded data, in terms of ground motion amplitude and P- and S-wave arrivals. The duration of recorded ground motions, however, appears to be longer than that of the simulated ones, which may be due to the scattering caused by small-scale heterogeneities that cannot be simulated by the one-dimensional layered model.

Ground motions of seven earthquakes originating from Heyuan, seven from Yangjiang and eight from Nanao have been simulated. The majority of the recorded ground motions could be simulated well, reflecting that the crustal model extracted from the CRUST 2.0 may represent the crustal structure of the coastal region. The results also prove the capability of the method used in the simulation, where small-magnitude earthquakes can be visualised as the Green's functions for large-magnitude earthquakes.

IDENTIFICATION OF POTENTIAL DISTANT EARTHQUAKES

Three historical intraplate earthquakes, namely the 1918 Nanao earthquake (M_w 7.3, R = 338 km), the 1962 Heyuan earthquake (M_w 6.1, R = 174 km) and the 1969 Yangjiang earthquake (M_w 6.4, R = 254 km), have affected Hong Kong. These earthquakes are the largest events in the respective regions that have occurred in the last 400 years. The onshore and offshore regions seem to exhibit differences in the seismic activities. In the onshore region, 80% of the earthquake activities are concentrated in two regions, namely Heyuan and Yangjiang. These regions have relatively higher seismic activities but the maximum earthquake magnitudes that can be generated are limited. The offshore region, on the other hand, is characterized by relatively fewer but larger earthquake events. It is therefore informative to estimate the ground motion intensities, in terms of response spectral velocity (RSV) across a wide range of natural period, that could generated by these historical earthquakes. This is a step towards understanding which cluster of distant intraplate earthquakes is the controlling scenario for the seismic hazard assessment of Hong Kong.

Earthquakes in Heyuan are mostly reservoir-triggered events, which are indicated by the dramatic increase in the seismic activities after the completion of a dam in the region in 1959. Most of the earthquakes are very small, but on 19 March 1962, a strong shock of magnitude 6.1 occurred. Since 1980, six earthquakes in this region have reportedly shaken high-rise buildings in Hong Kong to a perceptible level of vibration. The ground motion of the M_w 6.1 earthquake is to be simulated. The rupture area of the normal-slip earthquake is estimated to be 15 km × 9 km, using the empirical relationships proposed by Wells and Coppersmith [1994]. The fault is divided into 15 subfaults of 3 km × 3 km. The upper side of the fault is buried 200 m beneath the ground surface. The rupture is

Table II. Rupture models of the historical distant earthquakes.

	1962 Heyuan	1969 Yangjiang	1918 Nanao
M_w	6.1	6.4	7.3
R (km)	174	254	338
Strike (^{o})	N45E	N48E	N40E
Dip (^{o})	60	120	90
Rake (^{o})	-90 (normal)	180 (right-lateral)	180 (right-lateral)
Rupture area (km^2)	15 × 9 = 135	24 × 9 = 216	70 × 20 = 1400
Subfault size (km^2)	3 × 3 = 9	3 × 3 = 9	5 × 5 = 25
No. of subfaults	15	24	56
Hypocentre	Centre of fault	Centre of fault	Centre of fault
Asperity	No	No	No
Rupture velocity (km/s)	2.75	2.75	2.75
Slip (m)	0.417	0.735	2.235
Rise time (s)	1.30	1.57	3.33

Note: R is the epicentral distance measured from the headquarters of the HKO (22.3020^{o}N, 114.1743^{o}E).

assumed to start from the centre of the fault and it propagates radially throughout the fault plane with a velocity of 2.75 km/s. The amount of slips is taken to be uniform throughout the fault, and it is calculated to be 0.417 m to generate the M_w 6.1 event. Although the rupture model without asperity may not be realistic, it is used in this preliminary stage to determine which of the historical distant earthquakes may cause the greatest impact to Hong Kong. The rise time of the rupture of each subfault is taken to be 1.30 s, which is estimated using a stress drop of 100 bars [Somerville *et al*, 1987]. The strike and dip angles of the fault plane and the rake angle of the slip are N45^{o}E, 60^o and -90^o, respectively. These rupture properties are summarised in Table II.

The rupture models of the M_w 6.4 Yangjiang and M_w 7.3 Nanao earthquakes follow similar description as above, and they are also summarised in Table II. Unlike the Heyuan earthquake, the Yangjiang and Nanao earthquakes have right-lateral strike-slip focal mechanisms based on the tectonic setting described above.

Figure 4 compares the horizontal velocity time histories in Hong Kong simulated for the three earthquakes. The bedrock velocities generated by the Heyuan, Yangjiang and Nanao earthquakes are arranged from top to bottom, respectively. The horizontal ground motions are aligned to the radial and tangential directions, rather than to the NS and EW directions. The radial and tangential directions are more generic, in which the radial component mostly consists of the P, SV and Rayleigh waves, while the tangential component contains the SH and Love waves. The reference coordinate for Hong Kong is taken to be the headquarters of the HKO (22.3020^{o}N, 114.1743^{o}E). The upper cut-off frequency of the simulation is 2.0 Hz, and the time 0 s refers to the rupture initiation time. The peak ground velocity (PGV) is indicated in cm/s by the number at the top left corner of each panel. It is obvious that the PGV of the tangential component is larger than that of the radial one, in all three cases. The horizontal PGV, represented by the PGV in the tangential direction, of the Nanao earthquake (5.26 cm/s) is about three times that of the Yangjiang earthquake (1.73 cm/s) and about eight times that of the Heyuan earthquake (0.63 cm/s). The ground motion duration increases with the increase of the earthquake magnitude because the fault size increases so as the time needed for the whole rupture to take place.

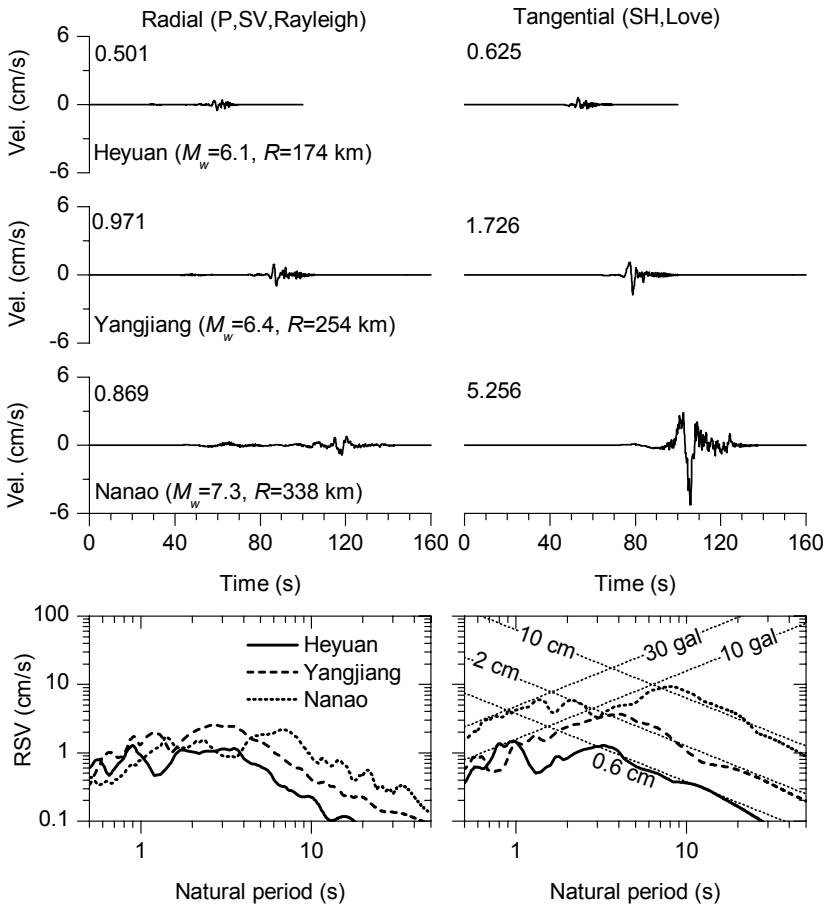

Figure 4. Horizontal ground velocities and velocity response spectra (5% damping ratio) of the Heyuan, Yangjiang and Nanao earthquakes.

The velocity response spectra (5% damping ratio) of the three earthquakes are compared in the bottommost panels of Figure 4. Note that the velocity response spectra in the present study are represented by their pseudo-velocity responses rather than the actual responses, as the former relate closely to the earthquake design spectrum usually specified in building codes [Chopra, 2001]. While the RSVs of Heyuan earthquake are comparable in both horizontal directions, the RSVs of Yangjiang and Nanao earthquakes in the tangential direction appear to be larger than those in the radial direction. Therefore, the tangential component may represent the horizontal direction in all three earthquakes. The RSA_{max}, RSV_{max} and RSD_{max} are defined as the maximum values of response spectral acceleration (RSA), velocity (RSV) and displacement (RSD), respectively, across the whole natural period range from 0.5 to 50 s. RSA_{max} of Nanao earthquake (30 cm/s^2 at natural periods T = 0.5 – 1.3 s) is three times that of Heyuan and Yangjiang earthquakes (10 cm/s^2 at T = 0.5 – 1.0 s). RSV_{max} of Nanao earthquake (9.2 cm/s at T = 8 s) is 2.5 times that of Yangjiang (3.7 cm/s at T = 4 s) and six times that of Heyuan (1.5 cm/s at T = 1 s). RSD_{max} of Nanao earthquake (10 cm T > 8 s) is five times that of Yangjiang (2 cm at T > 4 s) and 17 times that of Heyuan (0.6 cm at T > 3.5 s). This comparison indicates that the maximum spectral responses of Nanao earthquake are consistently larger than those of Yangjiang and Heyuan earthquakes. Therefore, the Nanao earthquake may be considered as the controlling earthquake of the intraplate distant earthquakes that may affect Hong Kong.

SIMULATION OF SCENARIO EARTHQUAKE IN NANAO

The de-aggregation of the UHS with 10% probability of exceedance over 50 years from the consultation study commissioned by the BD (referred to above) indicates that three scenario earthquakes are likely to give rise to the ground-motion hazards at short, medium and long natural-period ranges. An M_w 5.8 earthquake at 60 km from Hong Kong contributes most to the hazard level within a short natural-period range below 0.2 s, while earthquakes with M_w 6.3 at 100 km and M_w 7.4 at 340 km control the hazard levels within 0.2–1.0 s and above 1.0 s, respectively. The Nanao earthquake with an M_w of 7.4 may then be taken as the controlling earthquake for design of medium- to long-period structures (natural period ≥ 1 s) in Hong Kong. It is desirable to determine the credible response spectrum that may be generated by this earthquake taking into account the uncertainties in the rupture process. As the variance in the source parameters, such as rupture directivity, was not considered in the derivation of the UHS, the result obtained here may be used to refine the hazard spectrum.

Source Rupture Modelling

It is nearly impossible to accurately determine the source process of a future earthquake, but several parameters, such as the credible seismic moment, rupture area, strike and dip of the rupture plane, may be estimated with some degree of certainty. The rupture area of the Nanao earthquake with an M_w of 7.4 is estimated to be 85 km × 20 km using the empirical formula proposed by Wells and Coppersmith [1994]. The strike and dip of the fault plane are N40^{o}E and 90^o, respectively [Lin *et al*, 1980]. However, the other parameters, such as rupture directivity, slip distribution, presence of asperities, rupture velocity and dislocation rise-time, cannot be defined accurately. Therefore, they have to be treated as random values and constrained within a range of seismologically possible values.

Eighty random rupture models have been generated using a computer program developed for this study. The fault is divided into 68 subfaults of 5 km × 5 km. The rupture initiation may take place at any arbitrary location along the fault plane. To be realistic, the rupture may have two or three asperities with equal probability, where the total area of the asperities is confined to be 20% of the total rupture area. The slip contrast, which is defined as the ratio of the average slip in the asperity area to the average slip in total rupture area, is fixed at 2.0. These parameters are based on the analyses of fault asperities of fifteen earthquakes with M_w ranging from 5.7 to 7.2 [Somerville *et al*, 1999]. The individual asperities are randomly located along the fault plane without overlapping each other. The slips of the subfaults are lognormally distributed with a coefficient of variance (COV) of 0.2, where the slips of the total rupture area should produce an M_w 7.4 earthquake. The average slip of the asperity areas is computed to be 5.2 m, while that of the other subfaults is 1.9 m. The rake angle of the slip is random and is confined between 160^o and 200^o because the earthquake has a right-lateral strike-slip focal mechanism. The rupture propagates radially from the hypocentre with a constant velocity v_r, which may vary from 2 to 3 km/s for different rupture models. The dislocation rise-time of each subfault is calculated based on the empirical formula proposed by Somerville *et al* [1987], where the median value of the stress drop is taken to be 100 bars with a coefficient of variance of 0.2. The upper cut-off frequency of the simulation is 2.0 Hz.

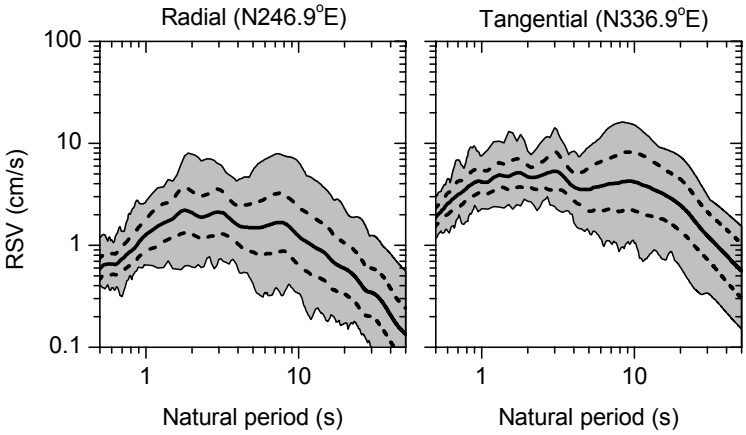

Figure 5. Velocity response spectra (5% damping ratio) of 80 random rupture models of the Nanao earthquake (M_w 7.4, R = 338 km).

Results

Figure 5 shows the velocity response spectra (5% damping ratio) in the radial and tangential directions of the ground motions in Hong Kong generated by the 80 random rupture models. The shaded areas indicate the ranges between the envelopes of the maximum and minimum spectra. The distribution of the spectral values agrees with the lognormal distribution, where the solid lines show the median spectra (50-percentile spectra), and the pairs of dashed lines mark the median-minus-one-standard-deviation (16-percentile) and median-plus-one-standard-deviation (84-percentile) spectra. The tangential spectrum is larger than the radial spectrum across the entire period range, thus the tangential spectrum may suitably represent the horizontal spectrum.

The variations in the spectral response shown in Figure 5 are the results of the uncertainties in the rupture process of the earthquake as assumed for the rupture parameters. It is obvious that the COV of the tangential RSV shown in Figure 5 is rather uniform, ranging around 0.28, up to a natural period of 2 s, after which the value increases continuously. At a natural period range of 8 – 11 s, the variance seems to have reached the maximum value of 0.66. It is also obvious from the maximum and minimum spectral envelopes that the components with a period of about 9 s are dominant in some cases but less dominant in others. It is desirable to analyse which rupture parameters are responsible for this long-period pulse.

Directivity Effects

Figures 6(a) and 6(b) show the rupture models of two extreme cases, where Model A produces large RSV at the natural period of 9 s, while Model B generates a relatively small value. Both rupture models are seismologically realistic models. The arrows in the figure show the slip vectors of the southeast block relative to the northwest one, viewed from the southeast. Both models have two asperities, which are marked in the figure by the shading. The solid circles denote the hypocentres, and the ruptures propagate radially at a velocity of 2.75 km/s for both models. In Model A, the two asperities are located southwest of the hypocentre, resulting to 79% of the seismic energy propagate toward southwest where Hong Kong is located and the remaining 21% propagate toward northeast. On the other hand, Model B has a hypocentre located at the southwest edge of the fault plane, implying that most of the seismic energy propagates away from Hong Kong. This directivity effect has a profound implication for the long-period ground motions generated in Hong Kong.

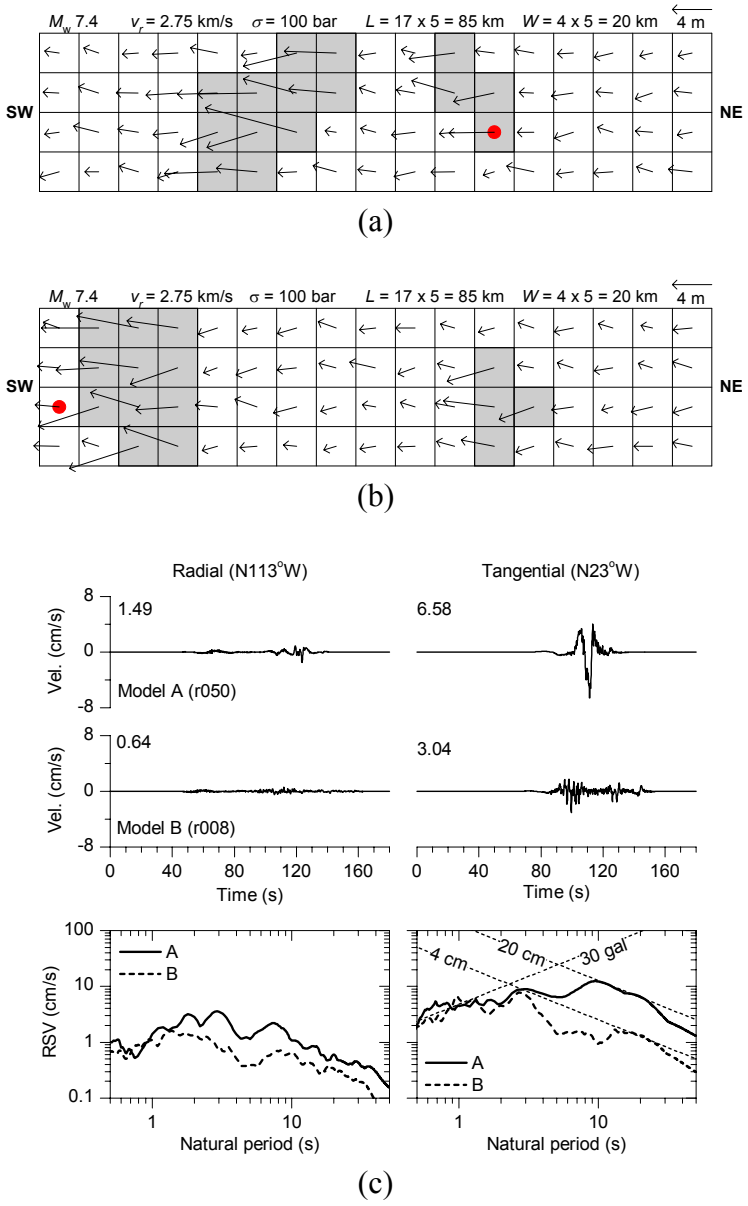

Figure 6. (a) Rupture Model A; (b) Rupture Model B; (c) Simulated ground velocities and velocity response spectra (5% damping ratio) of Models A and B.

Figure 6(c) compares the velocity time histories and velocity response spectra (5% damping ratio) of the two models. The numbers at the top-left corner of the time histories indicate the PGV in cm/s. The waveforms of Model A are different from those of Model B, where the most significant difference lies in the presence of an 9-s pulse (SH wave) in the tangential direction of Model A. The propagation of fault rupture toward Hong Kong at a velocity close to the shear wave velocity causes most of the seismic energy from the rupture to arrive in a single large pulse of motion that occurs at the beginning of the ground motion. This pulse is the result of the so-called forward rupture directivity where the rupture front propagates toward the site and the direction of the slip on the fault is oriented horizontally in the direction along the strike. Since the rupture of Model B propagates away from Hong Kong, it generates ground motion with smaller amplitude but longer duration. This is due to the so-called backward directivity effect. Because of the 9-s pulse, the PGV of Model A is more than twice that of

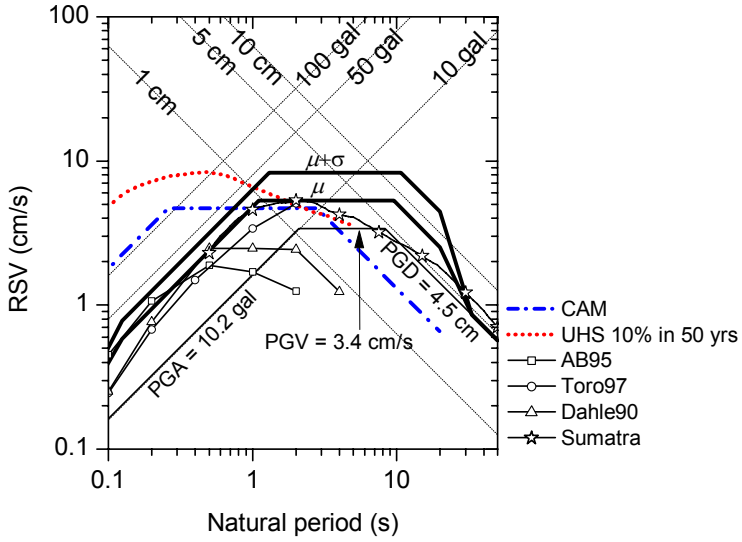

Figure 7. Elastic design spectrum of Nanao earthquake (M_w 7.4, R = 338 km).

Model B. Despite the large difference in PGV, the PGAs of the two models vary only moderately, namely 12.56 cm/s^2 for Model A and 10.76 cm/s^2 for Model B.

The rupture directivity effects seem to increase with the increase of natural period. The RSV in Figure 6(c) shows that the opposite rupture directivity in the two models causes insignificant variation in RSV up to a natural period of 3 s, after which the variation increases continuously up to a natural period of 10 s. The small variation of RSV for natural periods lower than 3 s shown in Figure 5 is therefore due to the difference in slip distribution as shown in Figures 6(a) and 6(b), rather than due to the rupture directivity itself. Although the values of RSA_{max} of the two models are similar (about 30 cm/s^2), due to the 9-s pulse, the RSV_{max} of Model A (12.4 cm/s) is 56% larger than that of Model B (7.9 cm/s), and the RSD_{max} of Model A (20 cm) is five times that of Model B (4 cm). The trend shown here is consistent with the directivity effects observed in the recorded near-field ground motions [Sommerville *et al*, 1997]. In the near field, however, the natural-period threshold where the directivity starts to show its effects is much lower at 0.6 s.

The ratios between the tangential and radial motions, in terms of PGV and RSV shown in Figure 6(c), range around 4 and seem to be independent of the rupture directivity. The ratios are primarily a function of radiation pattern, which depends on the source-site azimuth measured from the strike of the fault (26.9^o in this case).

Elastic Design Spectrum

The median spectrum in the tangential direction shown in Figure 5 is redrawn in a simpler format in Figure 7, where the jaggedness has been removed and the spectrum is represented by a series of straight lines. This smoothed spectrum is more appropriate for design purposes than that shown in Figure 5. The median values of PGA (10.2 cm/s^2), PGV (3.4 cm/s) and PGD (4.5 cm) are also plotted in Figure 7, implying amplification factors of 2.86, 1.56 and 1.78 for RSA_{max}, RSV_{max} and RSD_{max}, respectively, with respect to the peak amplitudes of the ground motion. The corner period T_1 at the intersection of the constant acceleration and constant velocity branches of the spectrum is 1.1 s, while the corner period T_2 where the constant velocity intersects the constant displacement is 9.5 s.

Table III. Description of four existing attenuation relationships derived for distant earthquakes.

Reference	Model notation	Data used	Model type[a]	Region type[b]	M_w[c]	R[d] (km)
Atkinson and Boore [1995]	AB95	Stochastically simulated ground motions in CENA	I	A	4.0 – 7.25	10 – 500
Toro *et al* [1997]	Toro97	Stochastically simulated ground motions in CENA	I	A	5.0 – 8.0	1 – 500
Dahle *et al* [1990]	Dahle90	Recorded ground motions of 56 intraplate earthquakes in North America, Europe, China and Australia	II	B	3.0 – 7.8	10 – 1000
Megawati *et al* [2003]	Sumatra	Stochastically simulated ground motions in Sumatra and the Malay Peninsula	I	B	4.0 – 8.0	170 – 1500

[a] Type I = attenuation model from curve fitting of stochastically simulated ground motions; Type II = attenuation model from curve fitting of recorded strong motions.
[b] Region A = stable continental region; Region B = active tectonic region.
[c] M_w indicates the range of moment magnitude considered.
[d] R indicates the range of source-to-station distance considered.

The earthquake intensities reported in Hong Kong during the 1918 Nanao earthquake ranged between VI and VII in the MMI scale. The PGV associated with this intensity range can be approximated using the relationship proposed by Newmark and Rosenblueth [1971]:

$$2^{\mathrm{MMI}} = 1.4 \times \mathrm{PGV\ (in\ mm/s)}$$

Thus, the MMI VI and VII correspond to PGV values of 4.57 cm/s and 9.14 cm/s, respectively. The median value of PGV simulated for the bedrock site is 3.4 cm/s. If the amplification factors of the local soil may be assumed ranging from 1.5 to 3, the bedrock motion predicted seems to be reasonable.

The UHS with 10% probability of exceedance in 50 years reported in the above-mentioned consultancy study commissioned by the BD is shown by the dotted line in Figure 7. As mentioned earlier, the scenario earthquake with M_w 7.4 at 340 km is expected to produce spectral values close to the UHS for periods longer than 1 s. However, the median spectrum exceeds the UHS for natural periods longer than 2 s. This is attributed to the elongation of the corner period T_2 of the median spectrum because of the rupture directivity effects. As the UHS is based on a point-source model, the effects of rupture directivity cannot be represented. If the directivity effect were removed from the median spectrum, T_2 of the median spectrum would reduce from 9.5 s to around 3 s (Figure 6), which would produce spectral values compatible the UHS. The effects of rupture directivity imply that the UHS for natural periods longer than 2 s is not conservative and should be increased to reflect the elongation of T_2. Further research is needed in order to fully quantify the degree of enhancement of long-period ground motions arising from directivity effects in far-field earthquakes.

The median spectrum is compared with the spectrum predicted by the Component Attenuation Model (CAM) in Figure 7 [Lam *et al*, 2002; Tsang and Chandler, 2004]. The $\mathrm{RSV_{max}}$ of both spectra agree well, but CAM predicts rather large $\mathrm{RSA_{max}}$ of 111 cm/s^2. Since CAM is based on a point-source

model, the effects of rupture directivity are also not represented. The agreement in the value of RSV_{max} predicted by CAM and that simulated in the present study is very encouraging, given that the methods used are fundamentally different.

Several attenuation relationships that have been developed considering distant earthquakes are summarised in Table III. The spectra predicted by these four attenuation relationships are plotted in Figure 7, and they show good agreement with the median spectrum of the present study in terms of RSA_{max}. The values of RSA_{max} predicted by the attenuation relationships range from 23 to 30 cm/s^2, and that of the median spectrum is 29 cm/s^2. Although the RSV_{max} predicted by AB95 and Dahle90 are only half the value of the median spectrum, the values predicted by Toro97 and Sumatra agree well with the median value. The first three attenuation relationships in Table III predict RSV only up to natural periods ranging from 2 to 4 s, thus they are unable to predict the long-period motions. Although the attenuation relationship of Sumatra was developed up to a natural period of 50 s, it cannot represent the long-period pulse of 9 s because it was derived using a point-source synthetic seismograms, which do not account for rupture directivity.

To be more conservative, the design spectrum can be represented by the median-plus-one-standard-deviation spectrum shown in Figure 7 as the $\sigma+\mu$ spectrum.

CONCLUSIONS

The potential earthquake in Nanao has been identified to be the most dominant far-field earthquake for Hong Kong. Ground motion of an M_w 7.4 earthquake in Nanao has been simulated, taking into account the uncertainties in the source rupture process. Traditionally, directivity effects are considered insignificant for distant earthquakes. However, the rupture directivity has been identified to be the main factor responsible for the formation of a large long-period pulse in the simulated ground motions. Due to this pulse, the spectral responses for natural periods longer than 2 s increase significantly, far exceeding the UHS. This means that the UHS is no longer conservative for natural periods longer than 2 s.

The most comprehensive seismic hazard assessment may be achieved through recursive analysis. The UHS is first obtained from a probabilistic analysis, after which the spectrum is de-aggregated to identify the dominant deterministic events giving rise to the ground-motion hazards at any particular natural periods of concern. More-sophisticated models of these events are then created to account for the variance in the source parameters, such as rupture directivity. The hazard analysis may then be repeated with the higher level of detail. The results of the present study are expected to serve the purpose of refining the seismic hazard levels of Hong Kong. The characteristics of the resulting ground motions may provide insights to the design considerations for long-period structures in Hong Kong and other regions facing similar problems. A suite of ground motions considering different rupture patterns have been simulated, and they will be useful for analysis of large structures such as long-span bridges and high-rise structures, for which the analysis is often done using time histories rather than response spectra to account for structural non-linearity.

ACKNOWLEDGEMENT

The authors would like to thank the Buildings Department of the Government of the Hong Kong Special Administrative Region (HKSAR) for their permission to allow the inclusion of selected results from their seismic hazard study. The work described was substantially supported by a grant from the Research Grants Council of the Hong Kong Special Administrative Region, China (Project No. HKU 7103/03E), whose support is gratefully acknowledged.

REFERENCES

Atkinson, G.M., Boore, D.M. (1995). Ground-motion relations for Eastern North America, *Bulletin of the Seismological Society of America* **85**, 17-30.

Chan, L.S. and Zhao, A. (1996). Frequency and time series analysis of recent earthquakes in the vicinity of Hong Kong, *Hong Kong Geologist* **2,** 11-19.

Chopra, A.K. (2001). Dynamics of Structures: Theory and Applications to Earthquake Engineering, Second Edition, Prentice Hall, Upper Saddle River, New Jersey, USA.

Dahle, A., Bungum, H., Kvamme, L.B. (1990). Attenuation models inferred from intraplate earthquake recordings. *Earthquake Engineering and Structural Dynamics* **19**, 1125-1141.

Fuchs, V.K. (1968). Das reflexions- und transmissionsvermogen eines geschichteten mediums mit beliebiger tiefen-verteilung der elastischen moduln und der dischte fur schragen einfall ebener wellen. *Zeitschrift für Geophysik* **34,** 389-413.

Geotechnical Control Office (1991). Review of earthquake data for the Hong Kong region. Geotechnical Control Office, Civil Engineering Service Department, Hong Kong, Publication No. 1.

Havskov, J. and Ottemöller, L. (2003). SeisAn: the earthquake analysis software, version 8.0. Department of Earth Science, The University of Bergen, Norway, website: http://www.ifjf.uib.no/seismo/software/seisan/seisan.html.

Kohketsu, K. (1985). The extended reflectivity method for synthetic near-field seismograms. *Journal of Physics of the Earth* **33:2,** 121-131.

Laske, G., Masters, G. and Reif, C. (2000). CRUST 2.0: A New Global Crustal Model at 2x2 Degrees. Institute of Geophysics and Planetary Physics, The University of California, San Diego, website: http://mahi.ucsd.edu/Gabi/rem.dir/crust/crust2.html.

Lam, N.T.K., Chandler, A.M., Wilson, J.L. and Hutchinson, G.L. (2002). Response spectrum predictions for potential near-field and far-field earthquakes affecting Hong Kong: rock sites. *Soil Dynamics and Earthquake Engineering* **22,** 47-72.

Lin, J., Liang, G., Zhao, Y. and Xie, M. (1980). Focal mechanism and tectonic stress field of coastal southeast China. *Acta Seismologica Sinica* **2:3,** 245-257.

Megawati, K., Pan, T.C., Koketsu, K. (2003). Response spectral attenuation relationships for Singapore and the Malay Peninsula due to distant Sumatran-fault earthquakes, *Earthquake Engineering and Structural Dynamics* **32,** 2241-2265.

Newmark, N.M. and Rosenblueth, E. (1971). Fundamental of Earthquake Engineering, Prentice-Hall, New Jersey, USA.

Pubellier, M. (1998). Geodynamic interpretations of the Sunda Block boundaries after GEODYSSEA results, *EOS Transaction*, AGU Fall Meeting.

Somerville, P.G., McLaren, J.P., LeFevre, L.V., Burger, R.W., Helmberger, D.V. (1987). Comparison of source scaling relations of eastern and western North American earthquakes. *Bulletin of the Seismological Society of America* **77**, 322-346.

Somerville, P.G., Smith, N.F., Graves, R.W. and Abrahamson, N.A. (1997). Modification of empirical strong ground motion attenuation relations to include the amplitude and duration effects of rupture directivity. *Seismological Research Letters* **68:1,** 199-222.

Somerville, P., Irikura, K., Graves, R., Sawada, S., Wald, D., Abrahamson, N., Iwasaki, Y., Kagawa, T., Smith, N. and Kowada, A. (1999). Characterizing crustal earthquake slip models for the prediction of strong ground motion. *Seismological Research Letters* **70:1,** 59-80.

Tam, C.M., Leung, Y.K., Pun, W.K., Fletcher, C.J.N. and Wilde, P.W. (1997). The new Hong Kong digital seismic monitoring network. *Hong Kong Geologist* **3,** 1-6.

Toro, G.R., Abrahamson, N.A., Schneider, J.F. (1997). Model of strong ground motions from earthquakes in Central and Eastern North America: best estimates and uncertainties, *Seismological Research Letters* **68**, 41-57.

Tsang, H.H., Chandler, A.M. (2004). Site-specific seismic hazard analysis in metropolitan cities: a Hong Kong case study. *Proceeding of the 3rd International Conference on Continental Earthquakes*, Beijing.

Wang, Z. and Lu, H. (1997). Evidence and dynamics for the change of strike-slip direction of the Changle-Nanao ductile shear zone, southeastern China. *Journal of Asian Earth Sciences* **15:6,** 507-515.

Wells, D.L. and Coppersmith, K.J. (1994). New empirical relationships among magnitude, rupture length, rupture width, rupture area, and surface displacement. *Bulletin of the Seismological Society of America* **84:4**, 974-1002.

Wilson, P., Rais, J. and Bakosurtanal, C. (1999). The GEODYSSEA Project: an investigation of the geology and geodynamics of South and Southeast Asia. *EOS* **79,** 545-548.